Chemical Science

ROYAL SOCIETY OF CHEMISTRY

EDGE ARTICLE

View Article Online
View Journal | View Issue

Cite this: *Chem. Sci.*, 2023, **14**, 4134

All publication charges for this article have been paid for by the Royal Society of Chemistry

Received 7th January 2023
Accepted 13th March 2023

DOI: 10.1039/d3sc00118k

rsc.li/chemical-science

Enantio- and diastereodivergent synthesis of fused indolizines enabled by synergistic Cu/Ir catalysis†

Bing-Ke Zhu,‡[ab] Hui Xu,‡[c] Lu Xiao,[a] Xin Chang,[a] Liang Wei,[a] Huailong Teng,[d] Yanfeng Dang,*[c] Xiu-Qin Dong*[a] and Chun-Jiang Wang*[ab]

Highly diastereo-/enantioselective assembly of 2,3-fused indolizine derivatives could be easily available through a cascade allylation/Friedel–Crafts type reaction enabled by a synergistic Cu/Ir catalysis. This designed protocol provides an unprecedented and facile route to enantioenriched indolizines bearing three stereogenic centers in moderate to high yields with excellent stereoselective control, which also featured broad substrate generality. Remarkably, four stereoisomers of the 2,3-fused indolizine products could be efficiently constructed in a predictable manner through the pairwise combination of copper and iridium catalysts. The synthetic utility of this method was readily elaborated by a gram-scale reaction, and synthetic transformations to other important chiral indolizine derivatives. Quantum mechanical explorations constructed a plausible synergetic catalytic cycle, revealed the origins of stereodivergence, and rationalized the protonation-stimulated stereoselective Friedel–Crafts type cyclization to form the indolizine products.

Introduction

The incorporation of stereogenic centers into privileged scaffolds to enhance the three-dimensional complexity represents a significant objective of chemical synthesis in support of pharmaceutical and materials science.[1] Indolizines, as one kind of important *N*-heterocycles, display an impressive range of bioactivities,[2] such as anticancer, antioxidant, antifungal, antiviral, and photophysical properties (Fig. 1).[3] The partially or fully reduced indolizine (mostly in enantiopure form) constitutes the core skeleton of over thousands of alkaloids.[4] The broad utilities of indolizine have long motivated the development of efficient methods for their preparation.

However, in comparison with the well-established non-asymmetric approaches, access to enantioenriched indolizines remains rare.[5] Successful catalytic asymmetric synthesis of chiral indolizine derivatives heavily relies on the Friedel–Crafts-type transformations with electrophiles to incorporate one stereogenic center on the C3-position of indolizine (Scheme 1a), including asymmetric conjugate addition, asymmetric propargylation and asymmetric allylic alkylation.[6] Recently, Feng, Liu, and coworkers developed an elegant diastereo-/enantioselective [3 + 2]-cycloaddition between pyridinium ylides and enones to deliver chiral tetrahydroindolizines, which could be easily oxidized to access high-value enantioenriched 3-arylindolizines with axial chirality.[7] Synthetic methods for other types of chiral indolizines, in particular, the privileged fused indolizine motifs have been rarely exploited. Therefore, a conceptually different strategy to achieve catalytic enantioselective functionalization of indolizine is urgently needed. On the other hand, the efficient generation of compound libraries with a broad stereochemical diversity is of great significance in both synthetic and medicinal chemistry.[8] In this aspect, the stereodivergent synthesis which involves the concurrent activation of two reactants *via* a dual organo-/metal, metal/metal or organo-/organo-catalysis is among the most effective methodologies.[9–11] In continuation of our longstanding interest in stereodivergent synthesis of α-amino acids,[9b,9d] we were intrigued by the possibility of π-allyl-Ir species derived from 2-

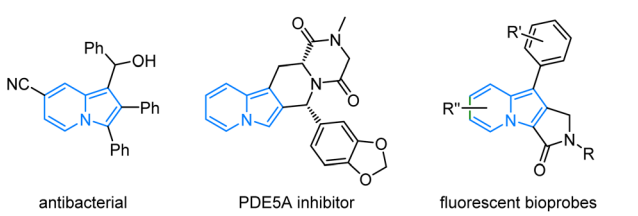

Fig. 1 Examples of bioactive compounds and organic fluorophores bearing indolizine heterocycles.

[a]*College of Chemistry and Molecular Sciences, Engineering Research Center of Organosilicon Compounds & Materials, Ministry of Education, Wuhan University, Wuhan, Hubei, 430072, P. R. China. E-mail: xiuqindong@whu.edu.cn; cjwang@whu.edu.cn*

[b]*State Key Laboratory of Organometallic Chemistry, Shanghai Institute of Organic Chemistry, Shanghai 230021, China*

[c]*Tianjin Key Laboratory of Molecular Optoelectronic Sciences, Department of Chemistry, Tianjin University, Tianjin 300072, China. E-mail: yanfeng.dang@tju.edu.cn*

[d]*College of Science, Huazhong Agricultural University, Wuhan, 430070, P. R. China*

† Electronic supplementary information (ESI) available. CCDC 2221435. For ESI and crystallographic data in CIF or other electronic format see DOI: https://doi.org/10.1039/d3sc00118k

‡ These two authors contributed equally.

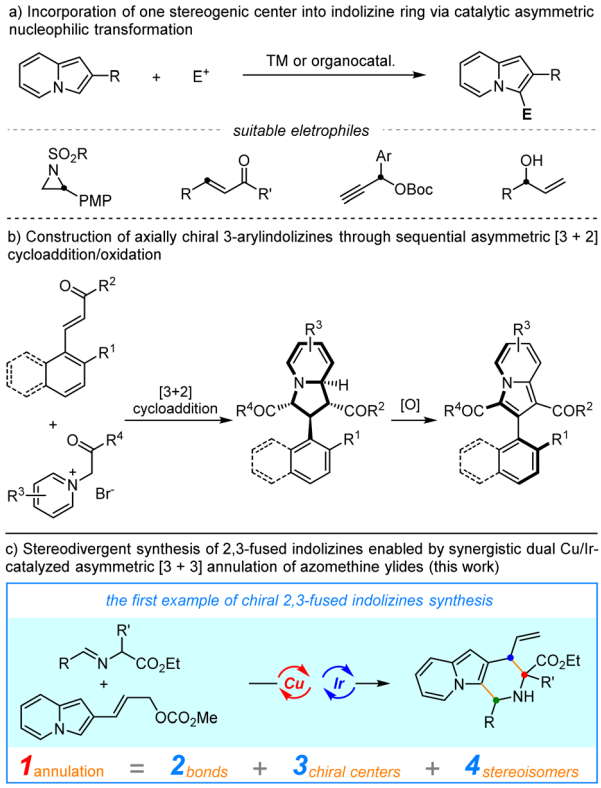

Scheme 1 Catalytic asymmetric synthesis of chiral indolizine derivatives.

indolizine allyl carbonates serving as 3-atom amphiphilic species in a cascade annulation with 1,3-dipolar-type metallated azomethine ylides. We anticipated that the addition of a nucleophilic Cu-azomethine ylides,[12] to such electrophilic π-allyl-Ir species followed by an intramolecular Friedel–Crafts-type annulation would provide a straightforward entry to chiral indolizines bearing three stereogenic centers. In addition, the high stereocontrol imparted by Ir catalysis on allylic alkylation[13] and Cu catalysis on α-functionalization of azomethine ylides might be able to control the generated stereogenic centers, thus allowing the precise construction of different stereoisomers of the 2,3-fused indolizines. Herein, we describe the first example of enantio-/diastereoselective synthesis of chiral indolizines *via* Cu/Ir-catalyzed asymmetric annulation through a cascade allylic alkylation/Friedel–Crafts reaction in high yields with excellent stereoselective control.

Results and discussion

Optimization of reaction conditions

To verify our hypothesis, a model reaction was conducted using *rac*-alanine ethyl ester derived aldimine ester **1a** and 2-indolizinyl allyl carbonate **2a** as the substrates, Cs_2CO_3 as the base, and dichloromethane as the solvent. As shown in Table 1, we first tested the catalytic efficiency of the combined [Cu(I)/(R,R_p)-**L1** + Ir(I)/(S,S_a)-**L5**] system which was used for the previous reactions

Table 1 Optimization of reaction conditions[a]

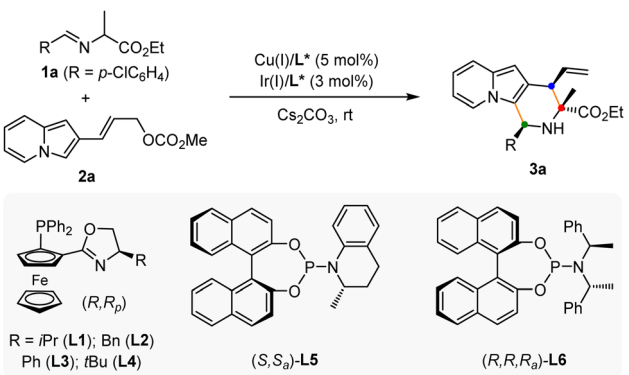

Entry	L* for Cu	L* for Ir	Solvent	dr[b]	Yield[c] (%)	ee[d] (%)
1	(R,R_p)-**L1**	(S_a,S)-**L5**	CH_2Cl_2	3 : 1	73	87
2	(R,R_p)-**L1**	(R_a,R,R)-**L6**	CH_2Cl_2	>20 : 1	93	99
3	(R,R_p)-**L2**	(R_a,R,R)-**L6**	CH_2Cl_2	19 : 1	83	97
4	(R,R_p)-**L3**	(R_a,R,R)-**L6**	CH_2Cl_2	>20 : 1	85	99
5	(S,S_p)-**L4**	(S_a,S,S)-**L6**	CH_2Cl_2	>20 : 1	87	99
6	(R,R_p)-**L1**	(R_a,R,R)-**L6**	THF	>20 : 1	85	99
7	(R,R_p)-**L1**	(R_a,R,R)-**L6**	Toluene	>20 : 1	87	99
8	(R,R_p)-**L1**	(R_a,R,R)-**L6**	EtOAc	>20 : 1	84	99
9	(R,R_p)-**L1**	(R_a,R,R)-**L6**	MeCN	19 : 1	80	97
10	(R,R_p)-**L1**	No Ir complex	CH_2Cl_2	—	NA	NA
11	No Cu complex	(R_a,R,R)-**L6**	CH_2Cl_2	—	NA	NA

[a] All reactions were carried out with 0.3 mmol **1a** and 0.2 mmol **2a** in 2 mL of solvent within 2–12 h. [b] dr was determined by the crude ^{1}H NMR analysis. [c] Yields refer to the isolated products after chromatographic purification. [d] ee was determined by chiral HPLC analysis.

Table 2 Reaction scope of Cu/Ir-catalyzed asymmetric [3 + 3] annulation[a]

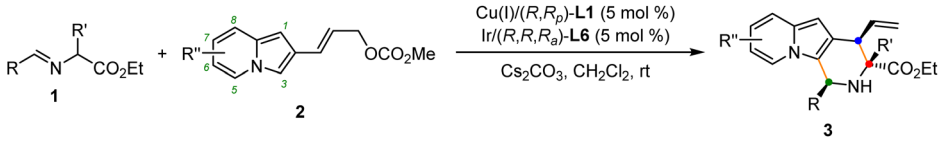

Entry	R	R′	R″	3	dr[b]	Yield[c] (%)	ee[d] (%)
1	*p*-ClC_6H_4	Me	H	**3a**	>20 : 1	93	99
2	*p*-BrC_6H_4	Me	H	**3b**	>20 : 1	85	99
3	*p*-FC_6H_4	Me	H	**3c**	>20 : 1	85	99
4	Ph	Me	H	**3d**	>20 : 1	88	99
5	*p*-MeC_6H_4	Me	H	**3e**	>20 : 1	95	99
6	*p*-$MeOC_6H_4$	Me	H	**3f**	>20 : 1	92	98
7	*m*-MeC_6H_4	Me	H	**3g**	>20 : 1	90	99
8	*m*-$MeOC_6H_4$	Me	H	**3h**	>20 : 1	91	99
9	*o*-MeC_6H_4	Me	H	**3i**	>20 : 1	87	99
10	1-Naphthyl	Me	H	**3j**	>20 : 1	86	99
11	2-Naphthyl	Me	H	**3k**	>20 : 1	95	99
12	2-Thenyl	Me	H	**3l**	>20 : 1	82	99
13	2-Furanyl	Me	H	**3m**	>20 : 1	86	99
14	*N*-Ts 3-indolyl	Me	H	**3n**	>20 : 1	90	99
15	Cyclohexyl	Me	H	**3o**	10 : 1	59	96
16	*n*-Bu	Me	H	**3p**	>20 : 1	60	99
17	*p*-ClC_6H_4	*n*-Bu	H	**3q**	>20 : 1	93	99
18	*p*-ClC_6H_4	i-Bu	H	**3r**	>20 : 1	88	99
19	*p*-ClC_6H_4	CH_2Ph	H	**3s**	>20 : 1	96	99
20	*p*-ClC_6H_4	CH_2CH_2Ph	H	**3t**	>20 : 1	85	99
21	*p*-ClC_6H_4	Allyl	H	**3u**	>20 : 1	96	99
22	*p*-ClC_6H_4	Cinnamyl	H	**3v**	>20 : 1	95	99
23	*p*-ClC_6H_4	CH_2CH_2SMe	H	**3w**	>20 : 1	97	99
24	*p*-ClC_6H_4	$CH_2CH_2CO_2Et$	H	**3x**	>20 : 1	91	99
25	*p*-ClC_6H_4	$(CH_2)_4NHCbz$	H	**3y**	>20 : 1	94	99
26	*p*-ClC_6H_4	3-Indolymethyl	H	**3z**	>20 : 1	55	99
27	*p*-$MeOC_6H_4$	H	H	**3A**	6 : 1	69	99
28	*p*-ClC_6H_4	Me	8-Me	**3B**	>20 : 1	83	99
29	*p*-ClC_6H_4	Me	7-Cl	**3C**	>20 : 1	82	99
30	*p*-ClC_6H_4	Me	6-Br	**3D**	>20 : 1	75	99
31	*p*-ClC_6H_4	Me	6-Ph	**3E**	>20 : 1	83	99

[a] All reactions were carried out with 0.3 mmol **1** and 0.2 mmol **2** in 2 mL of solvent within 2–12 h. [b] dr was determined by the crude ^{1}H NMR analysis. [c] Yields refer to the isolated products after chromatographic purification. [d] ee was determined by chiral HPLC analysis.

with 2-indolyl allyl carbonates.[11q,14] The reaction proceeded smoothly *via* the designed cascade allylation/Friedel–Crafts annulation pathway, giving (1*S*,3*R*,4*R*)-**3a** in 73% yield *albeit* with unsatisfactory diastereoselectivity and enantioselectivity (3 : 1 dr, 87% ee for the major isomer) (Table 1, entry 1). Although chiral phosphoramidite **L5** is privileged in our previous work,[11q] however, this reactivity and enantioselectivity on the allylic stereogenic center did not translate to 2-indolizinyl allyl carbonate. Encouragingly, using chiral phosphoramidite ligand (*R*,*R*,R_a)-**L6** (ref. 15) for the iridium catalyst instead of **L5**, the catalytic reactivity and stereoselective control were significantly enhanced, affording the desired product **3a** in 93% yield with >20 : 1 dr and 99% ee (Table 1, entry 2). No better results were achieved through the screening of a series of Phosferrox ligands[16] **L2–L4** for the copper catalyst (Table 1, entries 3–5). The effect of solvent was then tested, and dichloromethane provided the best results with a 93% yield among these solvents. No reaction was observed in the absence of either copper or iridium catalysts, which showed that both two chiral metal complexes are critical for this cascade allylation/Friedel–Crafts annulation to deliver the [3 + 3] annulation product (Table 1, entries 10–11).

Substrate scope study

The generality of the current protocol with respect to the azomethine ylide precursors was first examined under the established reaction conditions. As shown in Table 2, the scope of the substituted aldimine esters for this synergetic Cu/Ir-catalyzed asymmetric allylation/Friedel–Crafts type reaction was remarkably broad. A wide range of natural and unnatural amino acids derived aldimine esters underwent this cascade reaction with 2-indolizinyl allyl carbonates efficiently, giving the corresponding annulation products in good to high yields with excellent stereoselective control. The aromatic aldehyde derived α-methyl substituted aldimine esters (**1a–1i**) bearing substituents of

Table 3 Stereodivergent synthesis

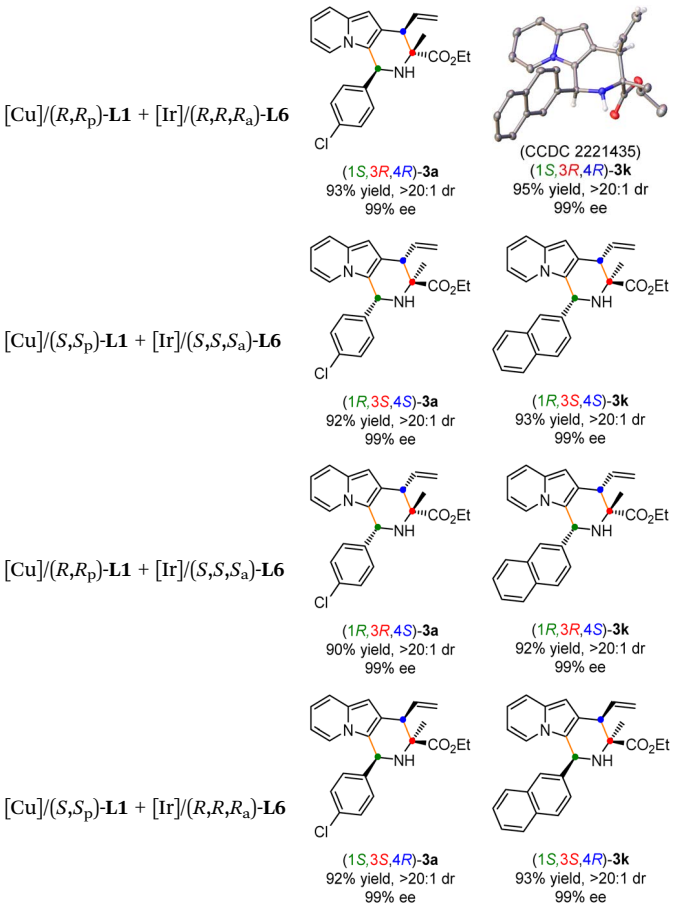

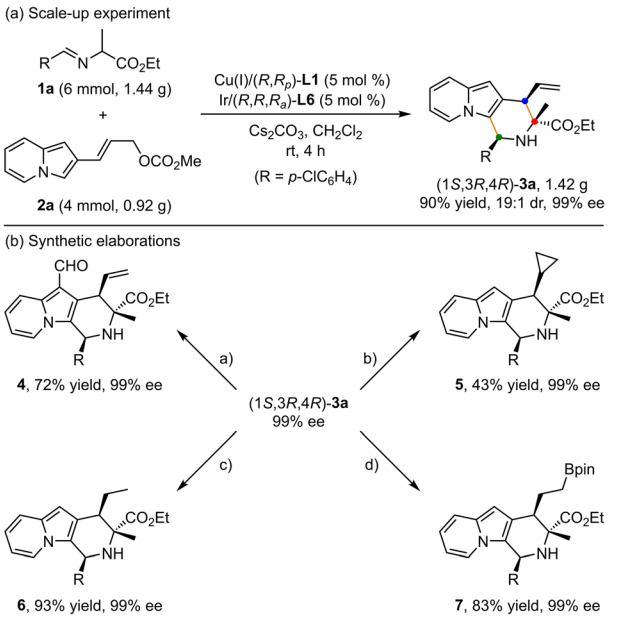

Scheme 2 Scale-up experiments and synthetic elaborations. Reaction conditions: (a) $POCl_3$, DMF, 0 °C; (b) $Pd(OAc)_2$ (1 mol%), CH_2N_2 Et_2O, −20 °C; (c) Pd/C, H_2, rt; (d) $[Ir(COD)Cl]_2$ (5 mol%), dppm (10 mol%), HBpin, DCM, rt.

different electronic properties on different positions participated in this reaction smoothly, affording the desired products (**3a–3i**) in 85–95% yields and generally >20 : 1 dr and 99% ee (Table 2, entries 1–9). In addition, the naphthyl substituted aldimine esters with steric hindrance also worked well to deliver the desired products **3j** and **3k** with excellent results (86% yield, >20 : 1 dr, 99% ee and 95% yield, >20 : 1 dr, 99%, respectively, entries 10 and 11). It's worth noting that the heteroaromatic substituted substrates containing 2-thenyl, 2-furanyl, and *N*-Ts 3-indolyl groups, were well compatible to generate the corresponding products **3l–3n** in 82–90% yields, >20 : 1 dr and 99% ee (entries 12–14). To our delight, the more challenging aliphatic aldehyde-derived aldimine esters **1o** and **1p** also can undergo this transformation smoothly, leading to the products **3o** and **3p** with excellent results (59% yield, 10 : 1 dr, 96% ee for **3o**, and 60% yield, >20 : 1 dr, 99% ee for **3p**, entries 15 and 16). Promoted by the success of α-methyl substituted aldimine esters in this cascade reaction, we then turned our attention to further investigating other α-substituted aldimine esters. When the methyl group was replaced by *n*-butyl (**1q**), i-butyl (**1r**), benzyl (**1s**), and phenylethyl (**1t**) groups, the corresponding aldimine esters worked well to give the desired products (**3q–3t**) with excellent results (85–96% yields, >20 : 1 dr, generally 99% ee, entries 17–20). Furthermore, we found that a series of aldimine esters containing α-functionalized substituted groups, such as allyl (**1u**), cinnamyl (**1v**), CH_2CH_2SMe (**1w**), CH_2CH_2-CO_2Et (**1x**), $(CH_2)_4NHCbz$ (**1y**) groups, could function as compatible substrates to provide products (**3u–3y**) in 91–97% yields with >20 : 1 dr and all with 99% ee (entries 21–25). Tryptophan-derived aldimine ester bearing α-3-indolymethyl (**1z**) with high steric hindrance worked well to give the corresponding cycloadduct **3z** in 55% yield with exclusive diastereoselectivity and excellent enantioselectivity (entry 26). Aldimine esters bearing sterically hindered α-substituted groups, such as isopropyl or cyclohexyl groups, did not work in this catalytic system. Remarkably, glycine-derived aldimine ester **1A**, which posed an additional challenge to control the stereoselectivity since the initially formed allylation intermediate still contains a readily-racemized proton, also reacted smoothly with **2a** affording desired product **3A** with satisfactory results (entry 27). To further expand the scope generality of this protocol, a variety of indolizine-derived allyl carbonates bearing varied substituents with different electronic properties were all well-tolerated in this synergistic Cu/Ir catalytic system, providing the highly functionalized indolizine derivatives (**3B–3E**) in moderate to good yields with excellent stereoselectivities (75–83% yields, all with >20 : 1 dr and 99% ee, entries 28–31).

Having established the optimal reaction conditions for the preparation of (1*S*,3*R*,4*R*)-**3a**, we began to evaluate the feasibility of stereodivergent synthesis *via* the synergistic Cu/Ir catalysis (Table 3). To our delight, the four stereoisomers of the indolizine derivative **3a** could be successfully prepared in high yields (90–93%) with exclusive diastereoselectivities and almost perfect enantioselectivities (all >20 : 1 dr and 99% ee) by simply switching the

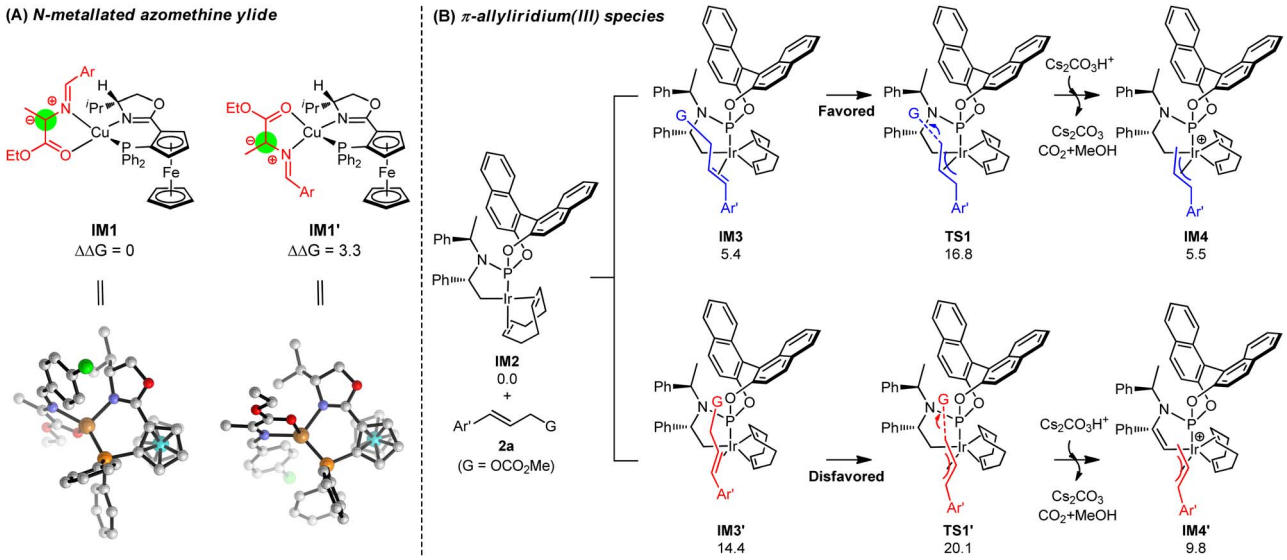

Fig. 2 (A) *In situ* generation and the structures of diastereomeric prochiral nucleophiles **IM1** and **IM1′**. (B) The generation of π-allyliridium(III) species **IM4** and **IM4′** *via* oxidative addition. Free energies are given in kcal mol^{-1}.

configuration combination of two chiral ligands **L1** and **L6** in the combined two chiral metal complexes. In addition, four stereoisomers of 2-naphthyl fused indolizine **3k** could be predictably achieved in the same manner. The absolute configuration of **3k** obtained with the combined [Cu(I)/(*R*,R_p)-**L1** + Ir(I)/(*R*,*R*,R_a)-**L5**] was unanimously determined to be (1*S*,3*R*,4*R*) by X-ray diffraction analysis (CCDC 2221435),[17] and the absolute configuration of other products was tentatively assigned by structural analogy.

Scale-up experiments and synthetic application

To showcase the synthetic utility of this methodology, first, a gram-scale of synergistic Cu/Ir-catalyzed asymmetric [3 + 3] annulation of alanine ethyl ester derived aldimine ester **1a** and 2-indolizinyl allyl carbonate **2a** was conducted (Scheme 2a), and the enantiopure 2,3-fused indolizine (1*S*,3*R*,4*R*)-**3a** could be smoothly achieved in 90% yield with 19 : 1 dr and 99% ee. As outlined in Scheme 2b, some synthetic transformations of (1*S*,3*R*,4*R*)-**3a** were further surveyed. It went through the Vilsmeier–Haack reaction efficiently to install a formyl group at the C1-position, providing the corresponding aldehyde compound **4** in 72% yield without any loss of enantioselectivity. The terminal alkenyl motif of product **3a** could react with CH_2N_2 catalyzed by $Pd(OAc)_2$ to generate product **5** containing the cyclopropane unit in moderate yield with maintained diastereoselectivity and enantioselectivity. In addition, Pd/C-catalyzed direct hydrogenation afforded product **6** in 93% yield without loss of diastereoselectivity. Moreover, the Ir/DPPM-catalyzed hydroboration of compound **3a** smoothly provided product **7** in 83% yield and without erosion of enantioselectivity.

Mechanistic studies

To gain insights into the molecular mechanism and understand the origins of stereoselectivity for this synergistic Cu/Ir catalysis, the catalytic reaction in entry 2, Table 1 (Cu/(*R*,R_p)-**L1** and Ir/(*R*,*R*,R_a)-**L6**) was chosen as a representative for DFT mechanistic study (see the ESI† for details). Fig. 2A exhibits the *in situ* generation of copper azomethine ylide (AY) nucleophiles **IM1** and **IM1′**. The metallated prochiral nucleophile has two diastereomers that show opposite relative orientations of the azomethine ylide unit with the ligand. The arrangement in which the large aryl group of the azomethine ylide unit is placed on the less encumbered left-hand side of the ligand is energetically favorable, which can be attributed to steric effects directed by the Cp-based group.[18] The diastereomeric **IM1′** is 3.3 kcal mol^{-1} less stable than **IM1** caused by steric hindrance. As a result, only the more stable diastereomer of the prochiral nucleophile **IM1** is considered in the following C–C coupling procedures.[18] Note that the formation of Cu(I)-azomethine ylide **IM1** *via* deprotonation by inorganic base Cs_2CO_3 is exergonic by −20.2 kcal mol^{-1}, indicating a strong thermodynamic driving force (see Fig. S3† for details).

In the meantime, the generation of the active π-allyliridium(III) species *via* decarboxylative oxidative addition was considered and the DFT-calculated results are presented in Fig. 2B. We explored an activated form of the Ir(I) catalyst **IM2**, which was produced from the activation of the C–H bond by Cs_2CO_3.[18d] In the presence of (*R*,*R*,R_a)-**L6**, the pathway of the formation of π-allyl-Ir(III) **IM4** (**IM2** → **IM3** → **TS1** → **IM4**) has overwhelming advantages in kinetics and thermodynamics than that leading to allyl-Ir(III) **IM4′** (**IM2** → **IM3′** → **TS1′** → **IM4′**). Specifically, the competition between **TS1** and **TS1′** shows a big energy barrier difference of 3.3 kcal mol^{-1} in support of π-allyl-iridium **IM4**, and **IM4** is more stable than its diastereomeric **IM1′** by 4.3 kcal mol^{-1}. The main reason for the energy differences lies in the binding mode of allyl carbonate **2a**, which gives rise to more steric hindrances between **2a** and the COD ligand in **IM3'**, **TS1'** and **IM4'** (see Fig. S4† for details). The computations coupled with the fact that the subsequent C–C coupling is relatively easy (see below) demonstrate that it is reasonable to consider **IM4** as the main active allyl-Ir(III) species derived from the oxidation process.

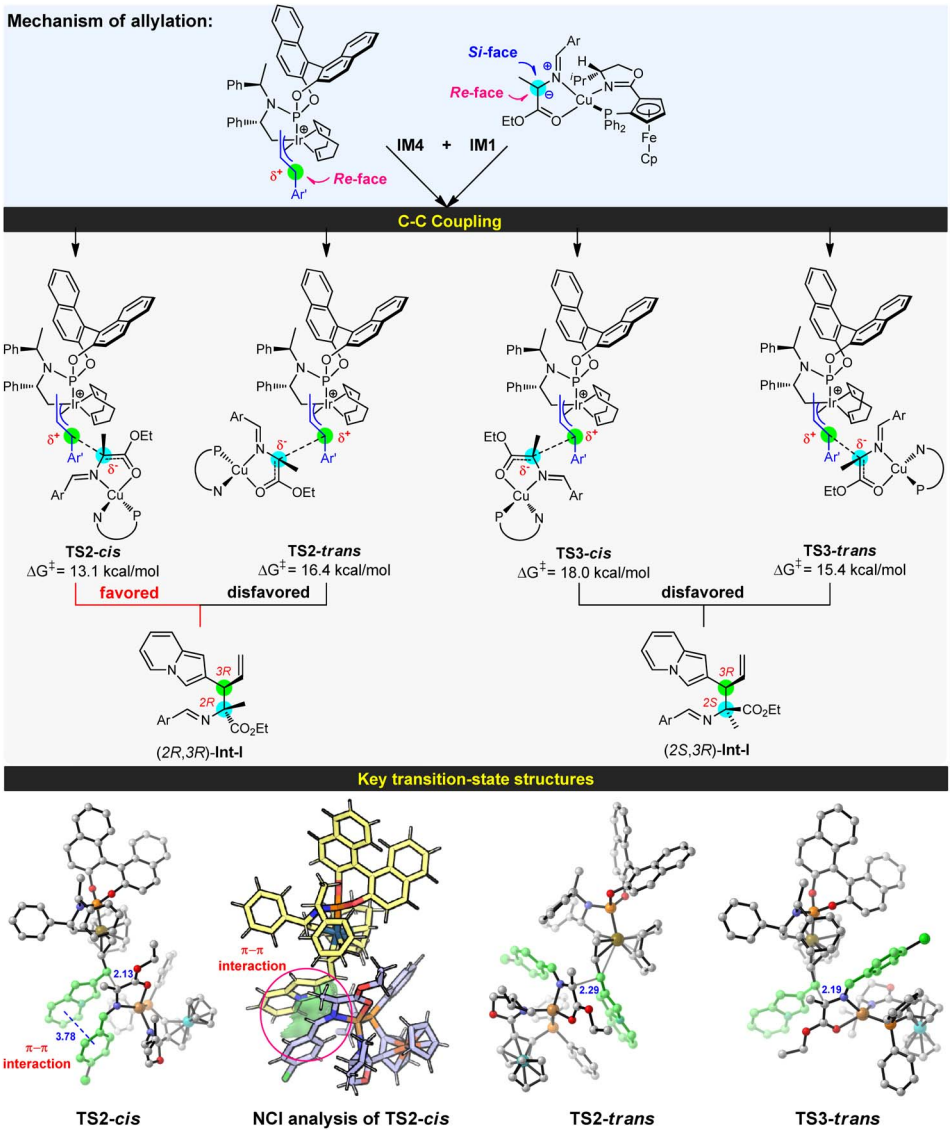

Fig. 3 Mechanism for the allylation of Cu(I)-azomethine ylide IM1 by allyliridium(III) IM4, and the key structures of bond-forming transition states. Free energies are given in kcal mol^{-1} (energy zero: IM1 and IM4), and selected distances are shown in Å.

With an in-depth investigation of the generation of the active Cu/Ir catalysis, we examined the C–C coupling of the nucleophilic Cu(I)-azomethine ylide **IM1** with the electrophilic allyl-iridium(III) **IM4** to disclose the stereoselectivity of two vicinal stereocenters (see Fig. 3). In the allyl-iridium(III) species **IM4**, the *Si*-face was hindered by the cyclometallated moiety and the COD ligand, and lost its reactivity towards the Cu(I)-ylide **IM1**. Correspondingly, the *Re*-face region was exposed and easily attacked by the nucleophile. As a result, the R-configuration of C4 in product **3a** can be preliminarily determined. On the other hand, in the Cu(I)-ylide **IM1**, the *Si*-face was congested by the oxazoline ring and its bulky isopropyl substituent; comparatively, the *Re*-face space was somewhat unimpeded and allowed the reaction with the electrophile. Hence, this indicated that the C3 site is more favored to be the R-configuration. On the basis of these analyses, we have located four types of C–C coupling transition states to form the alkylation compounds (see Fig. 3). **TS2-*cis*** originating from the reaction between the *Re*-face of **IM1** and the *Re*-face of **IM4** was the most favorable pathway and provided the allylation complex (2*R*,3*R*)-**Int-I**, which would undergo Friedel–Crafts type cyclization to give the experimental product (1*S*,3*R*,4*R*)-**3a** (see below). **TS2-*cis*** is 2.3 kcal mol^{-1} lower than **TS3-*trans***, the favored transition state to give the allylation complex (2*S*,3*R*)-**Int-I**, and the energy differences evidently support the formation of (2*R*,3*R*)-**Int-I** (>20 : 1 dr). As a result, the computationally predicted stereoselectivity is consistent with the experimental results (entry 2, Table 1). Herein, **TS2-*cis*** builds on the favorable *Re*-face–*Re*-face stereoscopic configuration with a *cis* Ar···Ar′ arrangement, which could avoid strong ligand/substrate steric repulsions and gain attractive π–π stacking interactions to stabilize the C–C coupling process. This type of π–π dispersion force was further verified by a visual analysis of non-covalent interactions (NCIs).[19] In the absence of this type of π–π interaction, **TS2-*trans*** has higher barrier than **TS2-*cis*** owing to the mismatched Ar···Ar′ structure. Additional *Re*-face–*Si*-face reaction

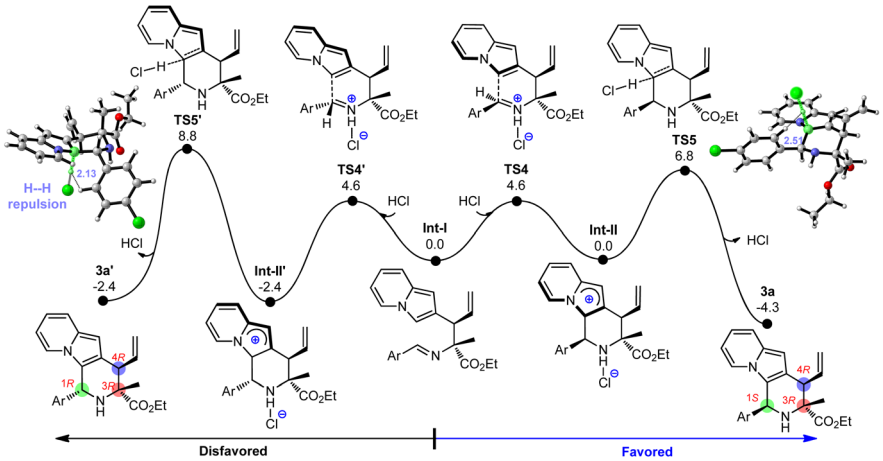

Fig. 4 Free energy profile for Friedel–Crafts type cyclization leading to the indolizine product **3a**.

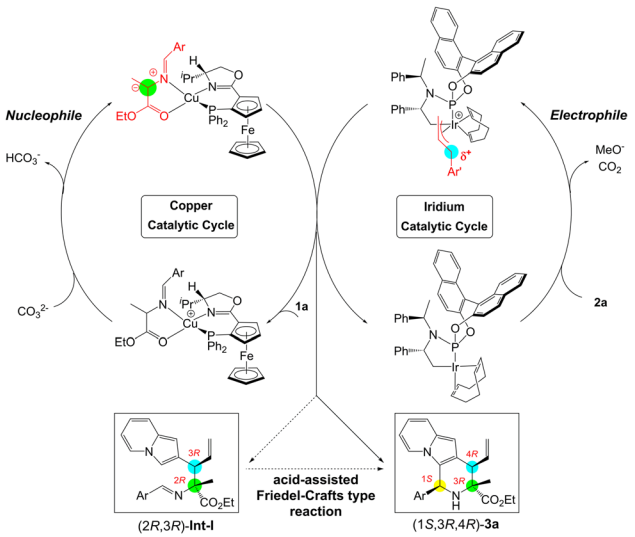

Scheme 3 Catalytic cycle for the cascade allylation/Friedel–Crafts type reaction *via* synergistic Cu/Ir catalysis.

pathways (**TS3**) enclosed strong steric hindrances between the allyl moiety and oxazoline fragment, so they are unfavorable (see Fig. S5† for details).

After revealing the formation of C3 and C4 stereocenters in product **3a** by Cu/Ir synergistic catalysis, we tried to understand the source of chirality at the C1 center. In view of the fact that catalytic amounts of protonic acids (*e.g.*, HCl) were generated during the catalyst activation (*e.g.*, **IM2**),[11q,18c] the protonated imine on the allylated intermediate **Int-I** can activate the electrophilic C=N bond and thus stimulate the ring-closure to yield the desired 2,3-fused indolizine product. Fig. 4 displays the DFT-computed free energy profile for the Friedel–Crafts type reaction, which consists of acid-enabled C–C bond formation (**TS4**) and base (Cl^-)-facilitated deprotonation (**TS5**). Because of the low kinetic barriers (4.6 kcal mol^{-1} and 6.8 kcal mol^{-1}) and favorable thermodynamic driving force (−4.3 kcal mol^{-1}), this Friedel–Crafts type cyclization is facile to carry out, which elucidates its high yield (93%, Table 1, entry 2). Although the energy barriers of C–C formation are similar (**TS4** *vs.* **TS4′**), **TS5** is 2.0 kcal mol^{-1} lower than **TS5′** during the deprotonation process, which illustrates the stereoselectivity favoring the (1*S*,3*R*,4*R*)-**3a** over (1*R*,3*R*,4*R*)-**3a**. The main factor that makes **TS5′** unstable is that it contains severe H···H steric repulsions labeled at 2.13 Å between the leaving H atom and the Ar group, while there is no H···H repulsion at the corresponding region in **TS5**. What's more, (1*R*,3*R*,4*R*)-**3a** has greater thermodynamic driving force than that of (1*S*,3*R*,4*R*)-**3a** (−4.3 kcal mol^{-1} *vs.* −2.4 kcal mol^{-1}), which is further conducive to the formation of product (1*S*,3*R*,4*R*)-**3a**. These analyses reveal the origins of stereochemistry. In addition, we explored the cascade allylation/Friedel–Crafts type reaction with the set of catalyst combination of (Cu(I)/(*S*,S_p)-**L1**+ Ir(I)/(*R*,*R*,R_a)-**L6**), and the computed results are analogous to those discussed above, and are in good agreement with the experimentally observed results in Table 3 (see Fig. S6–S7† for details).

As shown in Scheme 3, a reasonable cooperative catalytic cycle for this asymmetric cascade allylation/Friedel–Crafts type reaction to access enantioenriched 2,3-fused indolizine derivatives enabled by a synergistic Cu/Ir catalysis was established. This protocol could proceed through the asymmetric allylation between π-allyl-Ir(III) species derived from 2-indolizine allyl carbonates and Cu(I)-azomethine ylide, followed by a proton-assisted stereoselective Friedel–Crafts type cyclization to complete the annulation reaction and deliver the final 2,3-fused indolizine products.

Conclusions

In conclusion, we present herein a highly diastereoselective and enantioselective assembly of 2,3-fused indolizine derivatives empowered by a synergistic Cu/Ir catalysis with two readily available chiral ligands. The designed cascade allylation/Friedel–Crafts type reaction of *in situ*-formed nucleophilic Cu-azomethine ylides with electrophilic π-allyl-Ir species provides an unprecedented route to enantiomerically enriched indolizines bearing three stereogenic centers. The scope of this protocol, especially toward the aldimine esters, is remarkably broad. More importantly, through the pairwise combination of copper and iridium catalysts, this

method is capable of rapidly constructing four stereoisomers of the corresponding products in a predictable manner. DFT mechanistic studies established a reasonable cooperative catalytic cycle for the synergistic Cu/Ir catalysis to stereoselectively construct 2,3-fused indolizine derivatives bearing three stereogenic centers in moderate to high yields with excellent stereoselective control.

Data availability

All experimental procedures, characterisation data, mechanistic investigations, NMR spectra and HPLC spectra can be found in the ESI.†

Author contributions

C. J. W. conceptualized the project. C. J. W. and X. Q. D. supervised the investigation. B. K. Z., L. X., X. C. and L. W. performed the research. Y. D. directed the DFT calculation, and H. X. performed the DFT calculation research. C. J. W., X. Q. D. and Y. D. co-wrote the paper. All authors analyzed the data, discussed the results, and commented on the manuscript.

Conflicts of interest

There are no conflicts to declare.

Acknowledgements

This work was supported by NSFC (22071186, 22071187, 22073067, 22101216, and 22271226), National Youth Talent Support Program, Hubei Province NSF (2020CFA036 and 2021CFA069), and Fundamental Research Funds for the Central Universities (2042022kf1180).

Notes and references

1 F. Lovering, J. Bikker and C. Humblet, *J. Med. Chem.*, 2009, **52**, 6752–6756.

2 (*a*) V. Sharma and V. Kumar, *Med. Chem. Res.*, 2014, **23**, 3593–3606; (*b*) L.-L. Gundersen, A. H. Negussie, F. Rise and O. B. Østby, *Arch. Pharm.*, 2003, **336**, 191–195; (*c*) K. Bedjeguelal, H. Bienaymé, A. Dumoulin, S. Poigny, P. Schmitt and E. Tam, *Bioorg. Med. Chem. Lett.*, 2006, **16**, 3998–4001; (*d*) D. A. James, K. Koya, H. Li, S. Chen, Z. Xia, W. Ying, Y. Wu and L. Sun, *Bioorg. Med. Chem. Lett.*, 2006, **16**, 5164–5168; (*e*) Y. Xue, J. Tang, X. Ma, Q. Li, B. Xie, Y. Hao, H. Jin, K. Wang, G. Zhang, L. Zhang and L. Zhang, *Eur. J. Med. Chem.*, 2016, **115**, 94–108; (*f*) S. Park, E. H. Kim, J. Kim, S. H. Kim and I. Kim, *Eur. J. Med. Chem.*, 2018, **144**, 435–443.

3 (*a*) E. Kim, Y. Lee, S. Lee and S. B. Park, *Acc. Chem. Res.*, 2015, **48**, 538–547; (*b*) E. Kim, M. Koh, J. Ryu and S. B. Park, *J. Am. Chem. Soc.*, 2008, **130**, 12206–12207; (*c*) J. Li, S. Zhang and H. Zou, *Org. Chem. Front.*, 2020, **7**, 1218–1223; (*d*) W. E. Meador, S. A. Autry, R. N. Bessetti, J. N. Gayton, A. S. Flynt, N. I. Hammer and J. H. Delcamp, *J. Org. Chem.*, 2020, **85**, 4089–4095.

4 N. K. Ratmanova, I. A. Andreev, A. V. Leontiev, D. Momotova, A. M. Novoselov, O. A. Ivanova and I. V. Trushkov, *Tetrahedron*, 2020, **76**, 131031.

5 (*a*) G. S. Singh and E. E. Mmatli, *Eur. J. Med. Chem.*, 2011, **46**, 5237–5257; (*b*) S. Dong, X. Fu and X. Xu, *Asian J. Org. Chem.*, 2020, **9**, 1133–1143; (*c*) I. Khan, A. Ibrar and S. Zaib, *Top. Curr. Chem.*, 2021, **379**, 3; (*d*) J. S. S. Neto and G. Zeni, *Asian J. Org. Chem.*, 2021, **10**, 1282–1318.

6 (*a*) J. T. M. Correia, B. List and F. Coelho, *Angew. Chem., Int. Ed.*, 2017, **56**, 7967–7970; (*b*) H. Chen, L. Zhu, K. Zhong, X. Yue, L.-B. Qu, R. Bai and Y. Lan, *Chin. Chem. Lett.*, 2018, **29**, 1237–1241; (*c*) P.-J. Yang, L. Qi, Z. Liu, G. Yang and Z. Chai, *J. Am. Chem. Soc.*, 2018, **140**, 17211–17217; (*d*) L. Yang, X. Pu, D. Niu, Z. Fu and X. Zhang, *Org. Lett.*, 2019, **21**, 8553–8557; (*e*) K. Li and C. Li, *Org. Lett.*, 2020, **22**, 9456–9461; (*f*) P. Yang, C.-X. Liu, W.-W. Zhang and S.-L. You, *Acta Chim. Sin.*, 2021, **79**, 742–746; (*g*) J. Lu, M. Wang, R. Xu, H. Sun, X. Zheng, G. Zhong and X. Zeng, *Asian J. Org. Chem.*, 2021, **10**, 1500–1507; (*h*) Q. Ni, Z. Zhu, Y. Fan, X. Chen and X. Song, *Org. Lett.*, 2021, **23**, 9548–9553; (*i*) X. Song, Y. Fan, Z. Zhu and Q. Ni, *Org. Lett.*, 2022, **24**, 2315–2320.

7 D. Zhang, Z. Su, Q. He, Z. Wu, Y. Zhou, C. Pan, X. Liu and X. Feng, *J. Am. Chem. Soc.*, 2020, **142**, 15975–15985.

8 (*a*) J. Caldwell, *J. Clin. Pharmacol.*, 1992, **32**, 925–929; (*b*) B. Waldeck, *Chirality*, 1993, **5**, 350–355; (*c*) F. Lovering, J. Bikker and C. Humblet, *J. Med. Chem.*, 2009, **52**, 6752–6756; (*d*) K. M. Rentsch, *J. Biochem. Biophys. Methods*, 2002, **54**, 1–9; (*e*) K. Jozwiak, W. J. Lough and I. W. Wainer, *Drug Stereochemistry: Analytical Methods and Pharmacology*, 3rd edn, Informa, New York, 2012.

9 For perspectives and reviews on stereodivergent synergistic catalysis, see: (*a*) S. Krautwald and E. M. Carreira, *J. Am. Chem. Soc.*, 2017, **139**, 5627–5639; (*b*) L. Wei and C. J. Wang, *Chin. J. Chem.*, 2021, **39**, 15–24; (*c*) X. Huo, G. Li, X. Wang and W. Zhang, *Angew. Chem., Int. Ed.*, 2022, **61**, e202210086; (*d*) L. Wei and C.-J. Wang, *Chem. Catal.*, 2023, **3**, 100455.

10 For reviews on synergistic catalysis, see: (*a*) A. E. Allen and D. W. C. MacMillan, *Chem. Sci.*, 2012, **3**, 633–658; (*b*) Z. Du and Z. Shao, *Chem. Soc. Rev.*, 2013, **42**, 1337–1378; (*c*) D.-F. Chen, Z.-Y. Han, X.-L. Zhou and L.-Z. Gong, *Acc. Chem. Res.*, 2014, **47**, 2365–2377; (*d*) S. M. Inamdar, V. S. Shinde and N. T. Patil, *Org. Biomol. Chem.*, 2015, **13**, 8116–8162; (*e*) L. Lin and X. Feng, *Chem. - Eur. J.*, 2017, **23**, 6464–6482; (*f*) I. P. Beletskaya, C. Nájera and M. Yus, *Chem. Rev.*, 2018, **118**, 5080–5200; (*g*) Y. Wu, X. Huo and W. Zhang, *Chem.–Eur. J.*, 2020, **26**, 4895–4916; (*h*) U. B. Kim, D. J. Jung, H. J. Jeon, K. Rathwell and S.-g. Lee, *Chem. Rev.*, 2020, **120**, 13382–13433; (*i*) S. Martínez, L. Veth, B. Lainer and P. Dydio, *ACS Catal.*, 2021, **11**, 3891–3915; (*j*) X. Liu, H. Zheng, Y. Xia, L. Lin and X. Feng, *Acc. Chem. Res.*, 2017, **50**, 2621–2631.

11 For selected examples of stereodivergent synergistic catalysis, see: (*a*) S. Krautwald, D. Sarlah, A. Schafroth Michael and M. Carreira Erick, *Science*, 2013, **340**, 1065–1068; (*b*) S. Krautwald, M. A. Schafroth, D. Sarlah and

E. M. Carreira, *J. Am. Chem. Soc.*, 2014, **136**, 3020–3023; (*c*) T. Sandmeier, S. Krautwald, H. F. Zipfel and E. M. Carreira, *Angew. Chem., Int. Ed.*, 2015, **54**, 14363–14367; (*d*) X. Huo, R. He, X. Zhang and W. Zhang, *J. Am. Chem. Soc.*, 2016, **138**, 11093–11096; (*e*) F. A. Cruz and V. M. Dong, *J. Am. Chem. Soc.*, 2017, **139**, 1029–1032; (*f*) X. Huo, R. He, J. Fu, J. Zhang, G. Yang and W. Zhang, *J. Am. Chem. Soc.*, 2017, **139**, 9819–9822; (*g*) X. Huo, J. Zhang, J. Fu, R. He and W. Zhang, *J. Am. Chem. Soc.*, 2018, **140**, 2080–2084; (*h*) R. He, X. Huo, L. Zhao, F. Wang, L. Jiang, J. Liao and W. Zhang, *J. Am. Chem. Soc.*, 2020, **142**, 8097–8103; (*i*) Y. Peng, X. Huo, Y. Luo, L. Wu and W. Zhang, *Angew. Chem., Int. Ed.*, 2021, **60**, 24941–24949; (*j*) J. Zhang, X. Huo, J. Xiao, L. Zhao, S. Ma and W. Zhang, *J. Am. Chem. Soc.*, 2021, **143**, 12622–12632; (*k*) X. Jiang, J. J. Beiger and J. F. Hartwig, *J. Am. Chem. Soc.*, 2017, **139**, 87–90; (*l*) X. Jiang, P. Boehm and J. F. Hartwig, *J. Am. Chem. Soc.*, 2018, **140**, 1239–1242; (*m*) L. Wei, Q. Zhu, S.-M. Xu, X. Chang and C.-J. Wang, *J. Am. Chem. Soc.*, 2018, **140**, 1508–1513; (*n*) Z.-T. He, X. Jiang and J. F. Hartwig, *J. Am. Chem. Soc.*, 2019, **141**, 13066–13073; (*o*) M.-M. Zhang, Y.-N. Wang, B.-C. Wang, X.-W. Chen, L.-Q. Lu and W.-J. Xiao, *Nat. Commun.*, 2019, **10**, 2716; (*p*) Q. Zhang, H. Yu, L. Shen, T. Tang, D. Dong, W. Chai and W. Zi, *J. Am. Chem. Soc.*, 2019, **141**, 14554–14559; (*q*) S.-M. Xu, L. Wei, C. Shen, L. Xiao, H.-Y. Tao and C.-J. Wang, *Nat. Commun.*, 2019, **10**, 555; (*r*) S. Singha, E. Serrano, S. Mondal, C. G. Daniliuc and F. Glorius, *Nat. Catal.*, 2020, **3**, 48–54; (*s*) H. Wang, R. Zhang, Q. Zhang and W. Zi, *J. Am. Chem. Soc.*, 2021, **143**, 10948–10962; (*t*) M. Zhu, Q. Zhang and W. Zi, *Angew. Chem., Int. Ed.*, 2021, **60**, 6545–6552; (*u*) B. Kim, Y. Kim and S. Y. Lee, *J. Am. Chem. Soc.*, 2021, **143**, 73–79; (*v*) Y.-H. Wen, Z.-J. Zhang, S. Li, J. Song and L.-Z. Gong, *Nat. Commun.*, 2022, **13**, 1344; (*w*) S. Q. Yang, Y. F. Wang, W. C. Zhao, G. Q. Lin and Z. T. He, *J. Am. Chem. Soc.*, 2021, **143**, 7285–7291; (*x*) D. X. Zhu, J. G. Liu and M. H. Xu, *J. Am. Chem. Soc.*, 2021, **143**, 8583–8589; (*y*) L. Xiao, L. Wei and C. J. Wang, *Angew. Chem., Int. Ed.*, 2021, **60**, 24930–24940; (*z*) Y. Xu, H. Wang, Z. Yang, Y. Zhou, Y. Liu and X. Feng, *Chem*, 2022, **8**, 2011–2022; (*aa*) X. Chang, X. Cheng, X. T. Liu, C. Fu, W. Y. Wang and C. J. Wang, *Angew. Chem., Int. Ed.*, 2022, **61**, e202206517; (*ab*) R. Jiang, L. Ding, C. Zheng and S.-L. You, *Science*, 2021, **371**, 380–386; (*ac*) Q. Hu, Z. He, L. Peng and C. Guo, *Nat. Synth.*, 2022, **1**, 322–331; (*ad*) Z. He, L. Peng and C. Guo, *Nat. Synth.*, 2022, **1**, 393–400; (*ae*) L. Xiao, B. Li, F. Xiao, C. Fu, L. Wei, Y. Dang, X.-Q. Dong and C.-J. Wang, *Chem. Sci.*, 2022, **13**, 4801–4812; (*af*) L. Xiao, X. Chang, H. Xu, Q. Xiong, Y. Dang and C. J. Wang, *Angew. Chem., Int. Ed.*, 2022, **61**, e202212948; (*ag*) J. Han, R. Liu, Z. Lin and W. Zi, *Angew. Chem., Int. Ed.*, 2022, **61**, e202215714; (*ah*) W. Wang, F. Zhang, Y. Liu and X. Feng, *Angew. Chem., Int. Ed.*, 2022, **61**, e202208837; (*ai*) H. Wang, Y. Xu, F. Zhang, Y. Liu and X. Feng, *Angew. Chem., Int. Ed.*, 2022, **61**, e202115715; (*aj*) X. Hu, X. Tang, X. Zhang, L. Lin and X. Feng, *Nat. Commun.*, 2021, **12**, 3012; (*ak*) Y. Chen, Y. Liu, Z. Li, S. Dong, X. Liu and X. Feng, *Angew. Chem., Int. Ed.*, 2020, **59**, 8052–8056; (*al*) C. Xu, K. Wang, D. Li, L. Lin and X. Feng, *Angew. Chem., Int. Ed.*, 2019, **58**, 18438–18442; (*am*) H. Zheng, Y. Wang, C. Xu, Q. Xiong, L. Lin and X. Feng, *Angew. Chem., Int. Ed.*, 2019, **58**, 5327–5331; (*an*) S. Ge, W. Cao, T. Kang, B. Hu, H. Zhang, Z. Su, X. Liu and X. Feng, *Angew. Chem., Int. Ed.*, 2019, **58**, 4017–4021; (*ao*) Y. Chen, S. Dong, X. Xu, X. Liu and X. Feng, *Angew. Chem., Int. Ed.*, 2018, **57**, 16554–16558.

12 (*a*) L. Wei, X. Chang and C.-J. Wang, *Acc. Chem. Res.*, 2020, **53**, 1084–1100; (*b*) Z.-Y. Xue, Q.-H. Li, H.-Y. Tao and C.-J. Wang, *J. Am. Chem. Soc.*, 2011, **133**, 11757–11765; (*c*) H.-L. Teng, F.-L. Luo, H.-Y. Tao and C.-J. Wang, *Org. Lett.*, 2011, **13**, 5600–5603; (*d*) L. Wei, L. Xiao, Y. Hu, Z. Wang, H. Tao and C. Wang, *Chin. J. Org. Chem.*, 2019, **39**, 2119–2130.

13 Q. Cheng, H.-F. Tu, C. Zheng, J.-P. Qu, G. Helmchen and S.-L. You, *Chem. Rev.*, 2019, **119**, 1855–1969.

14 W. B. Liu, C. Zheng, C. X. Zhuo, L. X. Dai and S.-L. You, *J. Am. Chem. Soc.*, 2012, **134**, 4812–4821.

15 (*a*) J. F. Hartwig and L. M. Stanley, *Acc. Chem. Res.*, 2010, **43**, 1461–1475; (*b*) J. F. Teichert and B. L. Feringa, *Angew. Chem., Int. Ed.*, 2010, **49**, 2486–2528.

16 C. J. Richards and A. W. Mulvaney, *Tetrahedron: Asymmetry*, 1996, **7**, 1419–1430.

17 CCDC 2221435 ((1*S*,3*R*,4*R*)-**3k**) contains the supplementary crystallographic data for this paper.

18 (*a*) X.-X. Yan, Q. Peng, Y. Zhang, K. Zhang, W. Hong, X.-L. Hou and Y.-D. Wu, *Angew. Chem., Int. Ed.*, 2006, **45**, 1979–1983; (*b*) J. Xia, T. Hirai, S. Katayama, H. Nagae, W. Zhang and K. Mashima, *ACS Catal.*, 2021, **11**, 6643–6655; (*c*) H. Xu, B. Li, Z. Liu and Y. Dang, *ACS Catal.*, 2021, **11**, 9008–9021; (*d*) L. Xiao, B. Li, F. Xiao, C. Fu, L. Wei, Y. Dang, X.-Q. Dong and C.-J. Wang, *Chem. Sci.*, 2022, **13**, 4801–4812; (*e*) B. Li, H. Xu, Y. Dang and K. N. Houk, *J. Am. Chem. Soc.*, 2022, **144**, 1971–1985.

19 (*a*) S. Grimme, *Angew. Chem., Int. Ed.*, 2008, **47**, 3430–3434; (*b*) C. Lefebvre, G. Rubez, H. Khartabil, J.-C. Boisson, J. Contreras-García and E. Hénon, *Phys. Chem. Chem. Phys.*, 2017, **19**, 17928–17936; (*c*) A. J. Neel, M. J. Hilton, M. S. Sigman and F. D. Toste, *Nature*, 2017, **543**, 637–646.